Mode Matching for the Electromagnetic Scattering From Three-Dimensional Large Cavities

Gang Bao, Jinglu Gao, Junshan Lin, and Weiwei Zhang

***Abstract*—A new mode matching method is presented for the electromagnetic scattering from large cavity-backed apertures. The new method is based on the expansion of the field inside the cavity by the standard modes, and a periodic extension of the field on the cavity aperture to the whole ground plane. The computation cost is low by solving only the coefficients of the modes. Numerical examples are presented to show the efficiency of the approach.**

***Index Terms*—Electromagnetic scattering, large cavities, mode matching, radar cross section.**

I. Introduction

THE computation of the electromagnetic scattering from open cavities has received a lot of attention in recent years due to its important applications, such as the design of the jet inlet for an aircraft. For the cavities with the size of several wavelengths, standard techniques such as the method of moment (MoM) [7] or the finite element-boundary integral (FE-BI) approach ([8], [9]) have been developed to solve the problem efficiently. However, for three dimensional large cavities, in particular when the size of the cavity aperture is comparable to one hundred wavelengths or larger, such numerical methods are still too expensive even for supercomputers nowadays.

In fact, up to now there are basically two types of method to solve the scattering problem for very large cavities. The first type applies the high frequency asymptotic techniques. These include the Gaussian beam shooting [5], the bounding and shooting ray method ([13], [14]), etc. Another type of method expresses the field inside the cavity in terms of the waveguide modes. It is also known as the modal approach. Usually, the unknown modal coefficients are solved by the application of the reciprocity relationship and the Kirchhoff's approximation.

Manuscript received May 09, 2011; manuscript revised August 24, 2011; accepted September 26, 2011. Date of publication January 31, 2012; date of current version April 06, 2012. This work was supported in part by the National Science Foundation (NSF) under Grant DMS-0908325, Grant CCF-0830161, Grant EAR-0724527, and Grant DMS-0968360, in part by the Office of Naval Research (ONR) under Grant N00014-09-1-0384, and in part by a special research grant from Zhejiang University.

G. Bao is with the Department of Mathematics, Zhejiang University, Hangzhou, China. He is also with the Department of Mathematics, Michigan State University, East Lansing, MI 48824 USA (e-mail: bao@math.msu.edu).

J. Gao is with the School of Mathematics, Jilin University, Changchun 130012, China (e-mail: jinglugao@gmail.com).

J. Lin is with the Institute for Mathematics and Its Applications, University of Minnesota, Minneapolis, MN 55455 USA (E-mail: linxa011@ima.umn.edu).

W. Zhang is with the Department of Mathematics, King's College, Wilkes-Barre, PA 18711 USA (e-mail: weiweizhang@kings.edu).

Color versions of one or more of the figures in this paper are available online at http://ieeexplore.ieee.org.

Digital Object Identifier 10.1109/TAP.2012.2186255

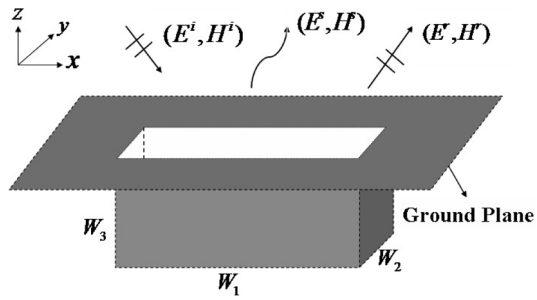

Fig. 1. Geometry of the cavity. The cavity is embedded in the ground plane.

We refer the reader to [1], [6], [11], [12], [14] and references therein for detailed discussions.

In the particular case when the cavity is very deep, a special higher order finite-element method is proposed that uses minimal memory ([10], [15]). We also refer to our recent numerical studies for the scattering from the two dimensional large open cavities by an improved mode matching method [4] and a finite difference scheme with fast algorithm [3]. For the rigorous study on the existence and uniqueness of the solution to the three dimensional scattering problem, we refer to [2].

In this paper, we present a mode matching approach for large cavities based on the periodic extension of the field on the cavity aperture to the whole ground plane. The method has the advantage of better accuracy for larger cavities. In particular, in the extreme case when the size of the cavity aperture goes to infinity, the numerical solution converges to the exact solution. In addition, it shares the low computational cost with the usual modal approach. Only the coefficient of the each mode is solved. Numerical examples are provided to illustrate the efficiency of the approach.

II. Formulation

Consider a time-harmonic (with $e^{-i\omega t}$ dependence) electromagnetic wave that impinges on the cavity backed aperture (Fig. 1). The rectangular cavity is embedded in the ground (the xy) plane, and both the cavity wall and the ground plane are assumed to be perfect conductors (PEC). The aperture of the cavity is $[-(W_1/2), W_1/2] \times [-(W_2/2), W_2/2]$, and the depth of the cavity is denoted as W_3. Here our attention is focused on the case when W_1 and W_2 are large.

Let ω be the frequency of the electromagnetic wave, and $k = \omega\sqrt{\epsilon_0\mu_0}$ be the wavenumber, where ϵ_0 and μ_0 are the permittivity and permeability of the vacuum respectively. The total electric and magnetic fields (E, H) consist of the incident wave (E^i, H^i), the reflected wave (E^r, H^r) by the ground plane and

the scattered wave (E^s, H^s). The governing equations for E and H are the Maxwell's equations

$$\begin{aligned}\nabla \times E - i\omega\mu H &= 0\\ \nabla \cdot (\epsilon E) &= 0\\ \nabla \times H + i\omega\epsilon E &= 0\\ \nabla \cdot (\mu H) &= 0.\end{aligned}$$

For clarity, the fields above the ground plane and inside the cavity are denoted by (E^+, H^+) and (E^-, H^-) respectively. By assuming that ϵ and μ are constant inside the cavity, the electric field E^- and the magnetic field H^- inside the cavity takes the following form:

$$\begin{aligned}E_x^- &= \sum_{m,n=0}^{\infty} a_{mn}\cos\left(\frac{m\pi}{W_1}x+\frac{m\pi}{2}\right)\sin\left(\frac{n\pi}{W_2}y+\frac{n\pi}{2}\right)\\ &\quad \sinh\left(\lambda_{mn}(z+W_3)\right),\\ E_y^- &= \sum_{m,n=0}^{\infty} b_{mn}\sin\left(\frac{m\pi}{W_1}x+\frac{m\pi}{2}\right)\cos\left(\frac{n\pi}{W_2}y+\frac{n\pi}{2}\right)\\ &\quad \sinh(\lambda_{mn}(z+W_3)),\\ E_z^- &= \sum_{m,n=0}^{\infty} c_{mn}\sin\left(\frac{m\pi}{W_1}x+\frac{m\pi}{2}\right)\sin\left(\frac{n\pi}{W_2}y+\frac{n\pi}{2}\right)\\ &\quad \cosh(\lambda_{mn}(z+W_3)),\end{aligned} \tag{1}$$

and

$$\begin{aligned}H_x^- &= \frac{1}{i\omega\mu}\sum_{m,n=0}^{\infty}\left(\frac{n\pi}{W_2}c_{mn}-\lambda_{mn}b_{mn}\right)\\ &\quad \sin\left(\frac{m\pi}{W_1}x+\frac{m\pi}{2}\right)\cos\left(\frac{n\pi}{W_2}y+\frac{n\pi}{2}\right)\\ &\quad \cosh(\lambda_{mn}(z+W_3)),\\ H_y^- &= \frac{1}{i\omega\mu}\sum_{m,n=0}^{\infty}\left(\lambda_{mn}a_{mn}-\frac{m\pi}{W_1}c_{mn}\right)\\ &\quad \cos\left(\frac{m\pi}{W_1}x+\frac{m\pi}{2}\right)\sin\left(\frac{n\pi}{W_2}y+\frac{n\pi}{2}\right)\\ &\quad \cosh(\lambda_{mn}(z+W_3)),\\ H_z^- &= \frac{1}{i\omega\mu}\sum_{m,n=0}^{\infty}\left(\frac{m\pi}{W_1}b_{mn}-\frac{n\pi}{W_2}a_{mn}\right)\\ &\quad \cos\left(\frac{m\pi}{W_1}x+\frac{m\pi}{2}\right)\cos\left(\frac{n\pi}{W_2}y+\frac{n\pi}{2}\right)\\ &\quad \sinh(\lambda_{mn}(z+W_3)).\end{aligned} \tag{2}$$

Here $\lambda_{mn} = \sqrt{(m\pi/W_1)^2 + (n\pi/W_2)^2 - w^2\epsilon\mu}$.

For the cavity with layered medium inside, a similar field representation can be derived. In each layer, E and H are expanded as the sum of the modes above, and the fields between two neighboring layers may be connected by the field continuity conditions.

Next, we calculate the fields (E^+, H^+) above the ground plane. By noting the PEC condition on the ground plane and the continuity of the electric field on the cavity aperture, it is easily seen that for the x and y components of the scattered field

$$\begin{cases} E_j^{s,+}(x,y,0) = E_j^-(x,y,0), & -\frac{W_1}{2}\le x\le\frac{W_1}{2}\\ & -\frac{W_2}{2}\le y\le\frac{W_2}{2}\\ E_j^{s,+}(x,y,0) = 0, & \text{elsewhere.}\end{cases}$$

where $j = x, y$. For conciseness, a function f defined over the cavity aperture is extended to the whole ground plane by introducing the operator $\mathcal{T}_0$ such that

$$\begin{cases}\mathcal{T}_0(f)(x,y) = f(x,y), & -\frac{W_1}{2}\le x\le\frac{W_1}{2}-\frac{W_2}{2}\le y\le\frac{W_2}{2}\\ \mathcal{T}_0(f)(x,y) = 0, & \text{elsewhere.}\end{cases}$$

Therefore, $E_j^{s,+}(x,y,0) = \mathcal{T}_0(E_j^-(x,y,0))$ for $j = x, y$.

From the Maxwell's equations, it is clear that the Fourier transform of the scattered field $E^{s,+}$ above the ground plane satisfies the equation

$$\frac{\partial^2\widehat{E_j^{s,+}}}{\partial z^2} + (k^2-\xi_1^2-\xi_2^2)\widehat{E_j^{s,+}} = 0, \quad j = x,y,z. \tag{3}$$

Here $\widehat{E_j^{s,+}}$ is the Fourier transform of the $E_j^{s,+}$ defined by

$$\widehat{E_j^{s,+}}(\xi_1,\xi_2,z) = \frac{1}{2\pi}\int_{\mathbb{R}^2} E_j^{s,+}(x,y,z)e^{-i(x\xi_1+y\xi_2)}dxdy.$$

By solving (3) with the radiation condition at infinity, the Fourier transform of the scattered field $E^{s,+}$ is the outgoing propagation modes expressed by

$$\widehat{E_j^{s,+}}(\xi_1,\xi_2,z) = e^{i\sqrt{k^2-\xi_1^2-\xi_2^2}z}\widehat{E_j^{s,+}}(\xi_1,\xi_2,0).$$

Hence, the scattered field $E^{s,+}$ above the ground plane are the inverse Fourier transforms

$$\begin{aligned}E_j^{s,+} &= \frac{1}{2\pi}\int_{\mathbb{R}^2} e^{i\sqrt{k^2-\xi_1^2-\xi_2^2}z}\widehat{E_j^{s,+}}(\xi_1,\xi_2,0)\\ &\quad e^{i(x\xi_1+y\xi_2)}d\xi_1 d\xi_2\\ &\quad j = x,y,z.\end{aligned}$$

For $j = x, y$, equivalently

$$\begin{aligned}E_j^{s,+} = \frac{1}{2\pi}\int_{\mathbb{R}^2} e^{i\sqrt{k^2-\xi_1^2-\xi_2^2}z}\widehat{\mathcal{T}_0(E_j^-)}(\xi_1,\xi_2,0)\\ e^{i(x\xi_1+y\xi_2)}d\xi_1 d\xi_2\end{aligned} \tag{4}$$

by noting that $E_j^{s,+}(x,y,0) = \mathcal{T}_0(E_j^-(x,y,0))$. When $j = z$, an application of the Gauss's law $\nabla\cdot E = 0$ above the ground plane implies that $E_z^{s,+}(x,y,z)$ can alternatively be written as

$$\begin{aligned}E_z^{s,+} = -\frac{1}{2\pi}\int_{\mathbb{R}^2}\frac{1}{\sqrt{k^2-\xi_1^2-\xi_2^2}}(\xi_1\widehat{\mathcal{T}_0(E_x^-)}(\xi_1,\xi_2,0)\\ +\xi_2\widehat{\mathcal{T}_0(E_y^-)}(\xi_1,\xi_2,0))e^{i(x\xi_1+y\xi_2+\sqrt{k^2-\xi_1^2-\xi_2^2}z)}d\xi_1 d\xi_2.\end{aligned} \tag{5}$$

For completeness, the derivation of (5) is provided in Appendix.

Therefore, by (4) and (5), the total magnetic field H^+ above the ground plane takes the following form:

$$\begin{aligned} H_x^+ &= \frac{1}{i\omega\mu_0}\left(\frac{\partial E_z^+}{\partial y}-\frac{\partial E_y^+}{\partial z}\right) \\ &= \frac{1}{i\omega\mu_0}\left(\frac{\partial E_z^i}{\partial y}-\frac{\partial E_y^i}{\partial z}\right)+\frac{1}{i\omega\mu_0}\left(\frac{\partial E_z^r}{\partial y}-\frac{\partial E_y^r}{\partial z}\right) \\ &\quad -\frac{1}{2\pi\omega\mu_0}\int_{\mathbb{R}^2}\Big\{\sqrt{k^2-\xi_1^2-\xi_2^2}\widehat{\mathcal{T}_0(E_y^-)}(\xi_1,\xi_2,0) \\ &\qquad +\frac{\xi_1\xi_2\widehat{\mathcal{T}_0(E_x^-)}(\xi_1,\xi_2,0)+\xi_2^2\widehat{\mathcal{T}_0(E_y^-)}(\xi_1,\xi_2,0)}{\sqrt{k^2-\xi_1^2-\xi_2^2}}\Big\} \\ &\quad e^{i(x\xi_1+y\xi_2+\sqrt{k^2-\xi_1^2-\xi_2^2}z)}d\xi_1 d\xi_2 \end{aligned} \tag{6}$$

$$\begin{aligned} H_y^+ &= \frac{1}{i\omega\mu_0}\left(\frac{\partial E_x^+}{\partial z}\right)-\frac{1}{i\omega\mu_0}\left(\frac{\partial E_z^+}{\partial x}\right) \\ &= \frac{1}{i\omega\mu_0}\left(\frac{\partial E_x^i}{\partial z}-\frac{\partial E_z^i}{\partial x}\right)+\frac{1}{i\omega\mu_0}\left(\frac{\partial E_x^r}{\partial z}-\frac{\partial E_z^r}{\partial x}\right) \\ &\quad +\frac{1}{2\pi\omega\mu_0}\int_{\mathbb{R}^2}\Big\{\sqrt{k^2-\xi_1^2-\xi_2^2}\widehat{\mathcal{T}_0(E_x^-)}(\xi_1,\xi_2,0) \\ &\qquad +\frac{\xi_1^2\widehat{\mathcal{T}_0(E_x^-)}(\xi_1,\xi_2,0)+\xi_1\xi_2\widehat{\mathcal{T}_0(E_y^-)}(\xi_1,\xi_2,0)}{\sqrt{k^2-\xi_1^2-\xi_2^2}}\Big\} \\ &\quad e^{i(x\xi_1+y\xi_2+\sqrt{k^2-\xi_1^2-\xi_2^2}z)}d\xi_1 d\xi_2. \end{aligned} \tag{7}$$

III. Mode Matching Method

The electric field E over the cavity aperture is extended periodically to the whole ground plane, i.e., the zero extension of the cavity modes $\mathcal{T}_0\left(\cos((m\pi/W_1)x+m\pi/2)\sin((n\pi/W_2)y+n\pi/2)\right)$ and $\mathcal{T}_0\left(\sin((m\pi/W_1)x+m\pi/2)\cos((n\pi/W_2)y+n\pi/2)\right)$ in (4)–(7) are replaced by the periodic functions $\cos((m\pi/W_1)x+m\pi/2)\sin((n\pi/W_2)y+n\pi/2)$ and $\sin((m\pi/W_1)x+m\pi/2)\cos((n\pi/W_2)y+n\pi/2)$ respectively on the whole ground plane. Such approximation has better accuracy with larger size of the cavity aperture. In the extreme case when the size of the cavity aperture goes to infinity, the approximation is exact.

Note that the Fourier transform of sine and cosine functions are given by

$$\begin{aligned} &\left[\sin\left(\frac{n\pi}{W_1}x+\frac{n\pi}{2}\right)\right]\widehat{\ } \\ &= \frac{i\sqrt{2\pi}}{2}\left(e^{-i(n\pi/2)}\delta\left(\xi_1+\frac{n\pi}{W_1}\right)-e^{i(n\pi/2)}\delta\left(\xi_1-\frac{n\pi}{W_1}\right)\right) \\ &\left[\cos\left(\frac{n\pi}{W_1}x+\frac{n\pi}{2}\right)\right]\widehat{\ } \\ &= \frac{\sqrt{2\pi}}{2}\left(e^{-i(n\pi/2)}\delta\left(\xi_1+\frac{n\pi}{W_1}\right)+e^{i(n\pi/2)}\delta\left(\xi_1-\frac{n\pi}{W_1}\right)\right) \end{aligned}$$

where δ is the standard Dirac delta function. Therefore, for the Fourier transform of the periodic extension of the cavity modes to whole ground plane, some simple calculations yield

$$\begin{aligned} &\int_{\mathbb{R}^2}\left[\sin\left(\frac{m\pi}{W_1}x+\frac{m\pi}{2}\right)\cos\left(\frac{n\pi}{W_1}y+\frac{n\pi}{2}\right)\right]\widehat{\ } \\ &\quad \sqrt{k^2-\xi_1^2-\xi_2^2}e^{i(x\xi_1+y\xi_2+\sqrt{k^2-\xi_1^2-\xi_2^2}z)}d\xi_1 d\xi_2 \\ &= 2\pi\nu_{mn}e^{i\nu_{mn}z}\sin\left(\frac{m\pi}{W_1}x+\frac{m\pi}{2}\right) \\ &\quad \cos\left(\frac{n\pi}{W_1}y+\frac{n\pi}{2}\right). \end{aligned} \tag{8}$$

$$\begin{aligned} &\int_{\mathbb{R}^2}\left[\cos\left(\frac{m\pi}{W_1}x+\frac{m\pi}{2}\right)\sin\left(\frac{n\pi}{W_1}y+\frac{n\pi}{2}\right)\right]\widehat{\ } \\ &\quad \frac{\xi_1\xi_2}{\sqrt{k^2-\xi_1^2-\xi_2^2}}e^{i(x\xi_1+y\xi_2+\sqrt{k^2-\xi_1^2-\xi_2^2}z)}d\xi_1 d\xi_2 \\ &= e^{i\nu_{mn}z}\frac{2\pi}{\nu_{mn}}\frac{m\pi}{W_1}\frac{n\pi}{W_2}\sin\left(\frac{m\pi}{W_1}x+\frac{m\pi}{2}\right) \\ &\quad \cos\left(\frac{n\pi}{W_1}y+\frac{n\pi}{2}\right). \end{aligned} \tag{9}$$

$$\begin{aligned} &\int_{\mathbb{R}^2}\left[\sin\left(\frac{m\pi}{W_1}x+\frac{m\pi}{2}\right)\cos\left(\frac{n\pi}{W_1}y+\frac{n\pi}{2}\right)\right]\widehat{\ } \\ &\quad \frac{\xi_2^2}{\sqrt{k^2-\xi_1^2-\xi_2^2}}\,e^{i(x\xi_1+y\xi_2+\sqrt{k^2-\xi_1^2-\xi_2^2}z)}\,d\xi_1 d\xi_2 \\ &= e^{i\nu_{mn}z}\frac{2\pi}{\nu_{mn}}\left(\frac{n\pi}{W_2}\right)^2\sin\left(\frac{m\pi}{W_1}x+\frac{m\pi}{2}\right) \\ &\quad \cos\left(\frac{n\pi}{W_1}y+\frac{n\pi}{2}\right). \end{aligned} \tag{10}$$

$$\begin{aligned} &\int_{\mathbb{R}^2}\left[\cos\left(\frac{m\pi}{W_1}x+\frac{m\pi}{2}\right)\sin\left(\frac{n\pi}{W_1}y+\frac{n\pi}{2}\right)\right]\widehat{\ } \\ &\quad \sqrt{k^2-\xi_1^2-\xi_2^2}\,e^{i(x\xi_1+y\xi_2+\sqrt{k^2-\xi_1^2-\xi_2^2}z)}\,d\xi_1 d\xi_2 \\ &= 2\pi\nu_{mn}e^{i\nu_{mn}z}\cos\left(\frac{m\pi}{W_1}x+\frac{m\pi}{2}\right) \\ &\quad \sin\left(\frac{n\pi}{W_1}y+\frac{n\pi}{2}\right). \end{aligned} \tag{11}$$

$$\begin{aligned} &\int_{\mathbb{R}^2}\left[\cos\left(\frac{m\pi}{W_1}x+\frac{m\pi}{2}\right)\sin\left(\frac{n\pi}{W_1}y+\frac{n\pi}{2}\right)\right]\widehat{\ } \\ &\quad \frac{\xi_1^2}{\sqrt{k^2-\xi_1^2-\xi_2^2}} \\ &\quad e^{i(x\xi_1+y\xi_2+\sqrt{k^2-\xi_1^2-\xi_2^2}z)}d\xi_1 d\xi_2 \\ &= e^{i\nu_{mn}z}\frac{2\pi}{\nu_{mn}}\left(\frac{m\pi}{W_1}\right)^2\cos\left(\frac{m\pi}{W_1}x+\frac{m\pi}{2}\right) \\ &\quad \sin\left(\frac{n\pi}{W_1}y+\frac{n\pi}{2}\right). \end{aligned} \tag{12}$$

$$\int_{\mathbb{R}^2}\left[\sin\left(\frac{m\pi}{W_1}x+\frac{m\pi}{2}\right)\cos\left(\frac{n\pi}{W_1}y+\frac{n\pi}{2}\right)\right]\widehat{\ }\,\frac{\xi_1\xi_2}{\sqrt{k^2-\xi_1^2-\xi_2^2}}e^{i(x\xi_1+y\xi_2+\sqrt{k^2-\xi_1^2-\xi_2^2}z)}d\xi_1 d\xi_2$$
$$=e^{i\nu_{mn}z}\frac{2\pi}{\nu_{mn}}\frac{m\pi}{W_1}\frac{n\pi}{W_2}\cos\left(\frac{m\pi}{W_1}x+\frac{m\pi}{2}\right)\sin\left(\frac{n\pi}{W_1}y+\frac{n\pi}{2}\right). \tag{13}$$

Here $\nu_{mn}=\sqrt{k^2-(m\pi/W_1)^2-(n\pi/W_2)^2}$.

By substituting (1), (8)–(13) into (6) and (7), finally on the cavity aperture $(x,y,0)$, the magnetic field

$$\begin{aligned}H_x^+ &= \frac{1}{i\omega\mu_0}\left(\frac{\partial E_z^i}{\partial y}-\frac{\partial E_y^i}{\partial z}\right)+\frac{1}{i\omega\mu_0}\left(\frac{\partial E_z^r}{\partial y}-\frac{\partial E_y^r}{\partial z}\right)\\ &\quad-\frac{1}{\omega\mu_0}\sum_{m,n=0}^{\infty}a_{mn}\sinh(\lambda_{mn}W_3)\left(\frac{1}{\nu_{mn}}\frac{m\pi}{W_1}\frac{n\pi}{W_2}\right)\\ &\quad\sin\left(\frac{m\pi}{W_1}x+\frac{m\pi}{2}\right)\cos\left(\frac{n\pi}{W_2}y+\frac{n\pi}{2}\right)\\ &\quad-\frac{1}{\omega\mu_0}\sum_{m,n=0}^{\infty}b_{mn}\sinh(\lambda_{mn}W_3)\\ &\quad\left(\frac{1}{\nu_{mn}}\left(\frac{n\pi}{W_2}\right)^2+\nu_{mn}\right)\\ &\quad\sin\left(\frac{m\pi}{W_1}x+\frac{m\pi}{2}\right)\cos\left(\frac{n\pi}{W_2}y+\frac{n\pi}{2}\right)\end{aligned} \tag{14}$$

$$\begin{aligned}H_y^+ &= \frac{1}{i\omega\mu_0}\left(\frac{\partial E_z^i}{\partial y}-\frac{\partial E_y^i}{\partial z}\right)\\ &\quad+\frac{1}{i\omega\mu_0}\left(\frac{\partial E_z^r}{\partial y}-\frac{\partial E_y^r}{\partial z}\right)\\ &\quad+\frac{1}{\omega\mu_0}\sum_{m,n=0}^{\infty}a_{mn}\sinh(\lambda_{mn}W_3)\left(\frac{1}{\nu_{mn}}(\frac{m\pi}{W_1})^2+\nu_{mn}\right)\\ &\quad\cos\left(\frac{m\pi}{W_1}x+\frac{m\pi}{2}\right)\sin\left(\frac{n\pi}{W_2}y+\frac{n\pi}{2}\right)\\ &\quad+\frac{1}{\omega\mu_0}\sum_{m,n=0}^{\infty}b_{mn}\sinh(\lambda_{mn}W_3)\left(\frac{1}{\nu_{mn}}\frac{m\pi}{W_1}\frac{n\pi}{W_2}\right)\\ &\quad\cos\left(\frac{m\pi}{W_1}x+\frac{m\pi}{2}\right)\sin\left(\frac{n\pi}{W_2}y+\frac{n\pi}{2}\right).\end{aligned} \tag{15}$$

In addition, $\left(\partial E_z^i/\partial y-\partial E_y^i/\partial z\right)+\left(\partial E_z^r/\partial y-\partial E_y^r/\partial z\right)$ and $\left(\partial E_z^i/\partial y-\partial E_y^i/\partial z\right)+\left(\partial E_z^r/\partial y-\partial E_y^r/\partial z\right)$ can be expanded as the sum of the corresponding modes. Now H^- and H^+ have the same mode expansion, the unknown coefficients a_{mn},b_{mn},c_{mn} are solved by imposing the continuity condition over the cavity aperture

$$H_x^+(x,y,0)=H_x^-(x,y,0),\quad H_y^+(x,y,0)=H_y^-(x,y,0)$$

and an application of the Gauss's law $\nabla\cdot E^-=0$. More precisely, for each fixed m and n, the coefficients a_{mn}, b_{mn} and c_{mn} are calculated by solving a 3×3 linear system, where the entries for the first two rows of the linear system are given by collecting the coefficients of the same modes in $H^-(x,y,0)$ and $H^+(x,y,0)$, and the entries for the last row are given by collecting the coefficients of the modes resulting from the Gauss's law $\nabla\cdot E^-=0$.

The advantage of the mode matching method over the traditional finite difference and finite element is apparent. We only need to calculate the coefficients a_{mn}, b_{mn} and c_{mn} by solving 3×3 linear system MN times, where $M=2W_1/\lambda$, $N=2W_2/\lambda$, and λ is the wavelength. The calculation may be easily accelerated in a parallel way.

The mode matching solution is convergent in the sense of the distribution. That is, $\langle E_m^- - E^-,\phi\rangle\to 0$ for any smooth function ϕ when both W_1 and W_2 go to infinity. Here E_m^- represents the mode matching solution and E^- is the exact electric field.

To calculate the scattered far field, the modal coefficients a_{mn},b_{mn},c_{mn} are substituted back to the formulas (1), (4) and (5). By the method of stationary phase [16], at point (r,θ,ϕ) in spherical coordinate, asymptotically the scattered field is given by

$$\begin{aligned}E_x^{s,+} &= ik\cos\theta\widehat{\mathcal{T}_0(E_x^-)}(k\sin\theta\cos\phi,k\sin\theta\sin\phi,0)\,\frac{e^{ikr}}{r}\\ &\quad+O\left(\frac{1}{r^2}\right),\\ E_y^{s,+} &= ik\cos\theta\widehat{\mathcal{T}_0(E_y^-)}(k\sin\theta\cos\phi,k\sin\theta\sin\phi,0)\,\frac{e^{ikr}}{r}\\ &\quad+O\left(\frac{1}{r^2}\right),\\ E_z^{s,+} &= -ik\,(\sin\theta\cos\phi\widehat{\mathcal{T}_0(E_x^-)}(k\sin\theta\cos\phi,k\sin\theta\sin\phi,0)\\ &\quad+\sin\theta\sin\phi\widehat{\mathcal{T}_0(E_x^-)}(k\sin\theta\cos\phi,k\sin\theta\sin\phi,0))\,\frac{e^{ikr}}{r}\\ &\quad+O\left(\frac{1}{r^2}\right).\end{aligned}$$

The Fourier transforms $\widehat{\mathcal{T}_0(E_x^-)}$ and $\widehat{\mathcal{T}_0(E_y^-)}$ can be evaluated easily since the integrals are defined on the cavity aperture $[-(W_1/2),W_1/2]\times[-(W_2/2),W_2/2]$.

IV. Numerical Results

Several numerical results are presented to demonstrate the efficiency of the new mode matching method. The incident wave

$$E^i(r)=(\cos\alpha\hat{\theta}+\sin\alpha\hat{\phi})e^{ikd\cdot r}$$

where α is the polarization angle, $\hat{\theta}$ and $\hat{\phi}$ are the standard unit vectors in the spherical coordinate, and d is the incident direction given by

$$d=-(\sin\theta\cos\phi,\sin\theta\sin\phi,\cos\theta).$$

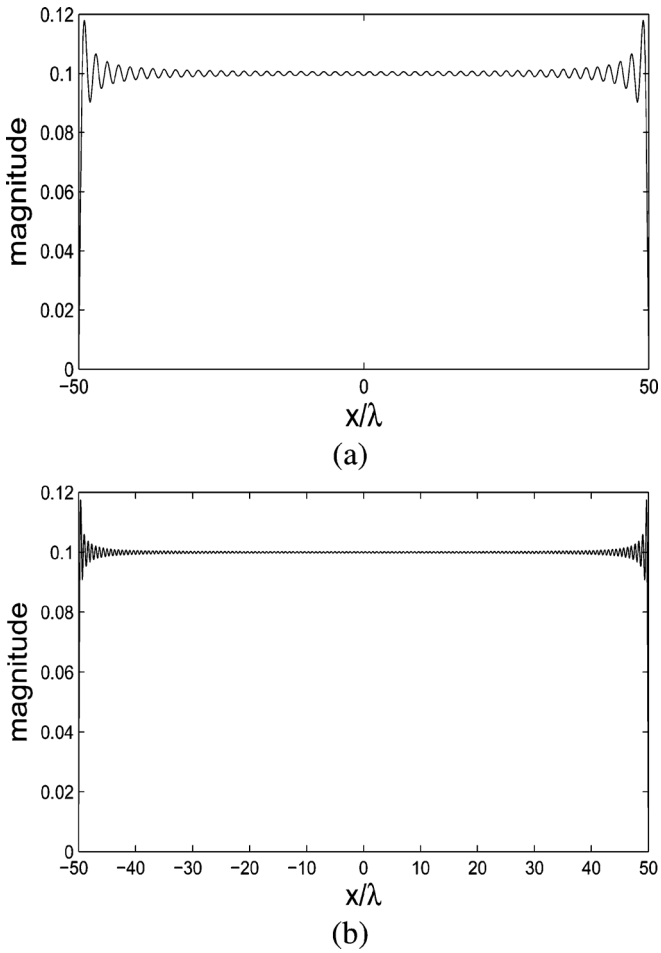

Fig. 2. (a) Magnitude of the electric field for $y = 0$ when 100 modes are used; (b) the magnitude when 300 modes are used.

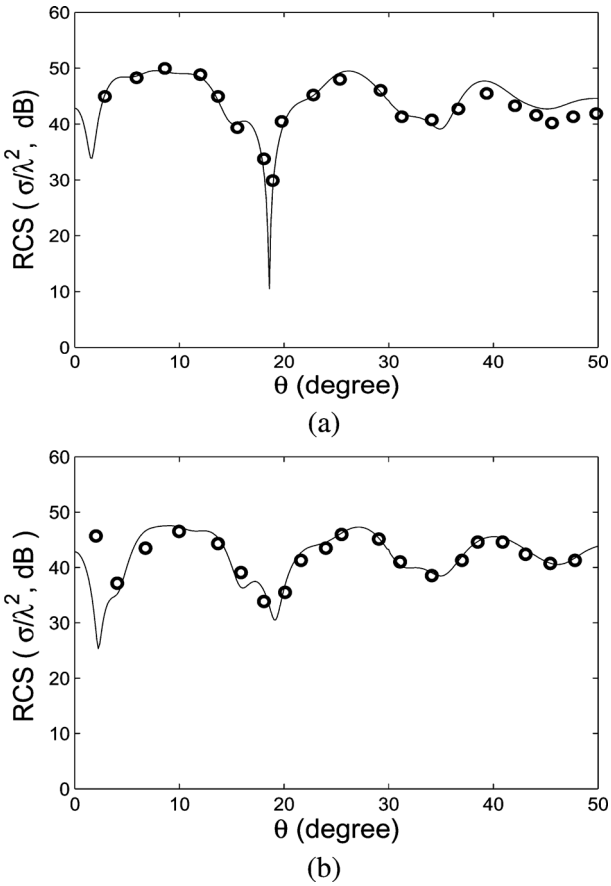

Fig. 3. RCS of the cavity with size $W_1 = W_2 = 10\lambda$, and $W_3 = 30\lambda$. $\phi = 0$ (xz plane). The solid line is the RCS calculated by the new mode matching method, and the circle is the RCS calculated by the modal approach presented in [14]. (a): $\hat{\phi}\hat{\phi}$ polarization; (b): $\hat{\theta}\hat{\theta}$ polarization.

First, we consider a normal ($\theta = 0$) incident wave with $\hat{\theta}$ polarization that impinges on a wide and shallow cavity. The wavenumber $k = 2\pi$, $W_1 = W_2 = 100\lambda$ and $W_3 = \lambda/(40\pi)$. In this case, the scattering from the cavity becomes a total reflection problem. Thus the exact magnitude $|E| \approx 2\sin(kW_3) \approx 0.1$ over the cavity aperture. We employ the new mode matching method to calculate the electric field E. Two different numbers of modes are used, and the corresponding magnitude of the electric field over the capture is plotted for $y = 0$ (Fig. 2). It is clear that the magnitude of the numerical solution converges to the magnitude of the exact electric field $|E|$ over the cavity aperture as the number of the mode increases.

Next, the backscatter radar cross section (RCS) of the cavity with size $W_1 = W_2 = 10\lambda$, and $W_3 = 30\lambda$ is calculated. The same example is also presented in [14]. When $\phi = 0$, the RCS of the $\hat{\phi}\hat{\phi}$ and $\hat{\theta}\hat{\theta}$ polarizations are shown for various incident angles θ in Fig. 3. Other than the first 5 degrees for the $\hat{\theta}\hat{\theta}$ polarization and the last 5 degrees for the $\hat{\phi}\hat{\phi}$ polarizations, the numerical result shows excellent agreement with the calculations by the modal approach presented in [14]. The RCS of the cavity when $\phi = \pi/4$ is also calculated for various incident angles, and the comparison with the calculations in [14] is shown in Fig. 4. The agreement between the two approaches is also excellent for $\theta \in (5, 50)$.

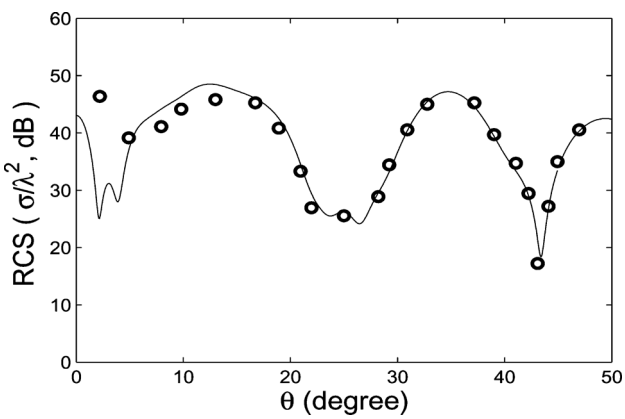

Fig. 4. RCS of the cavity with size $W_1 = W_2 = 10\lambda$, and $W_3 = 30\lambda$ ($\hat{\theta}\hat{\theta}$ polarization). $\phi = \pi/4$. The solid line is the RCS calculated by the new mode matching method, and the circle is the RCS calculated by the modal approach presented in [14].

The last example considers the scattering from a cavity of extreme large size with $W_1 = 20\lambda$, $W_2 = 60\lambda$, and $W_3 = 50\lambda$. Fig. 5 shows the backscatter RCS for the $\hat{\phi}\hat{\phi}$ and $\hat{\theta}\hat{\theta}$ polarizations respectively.

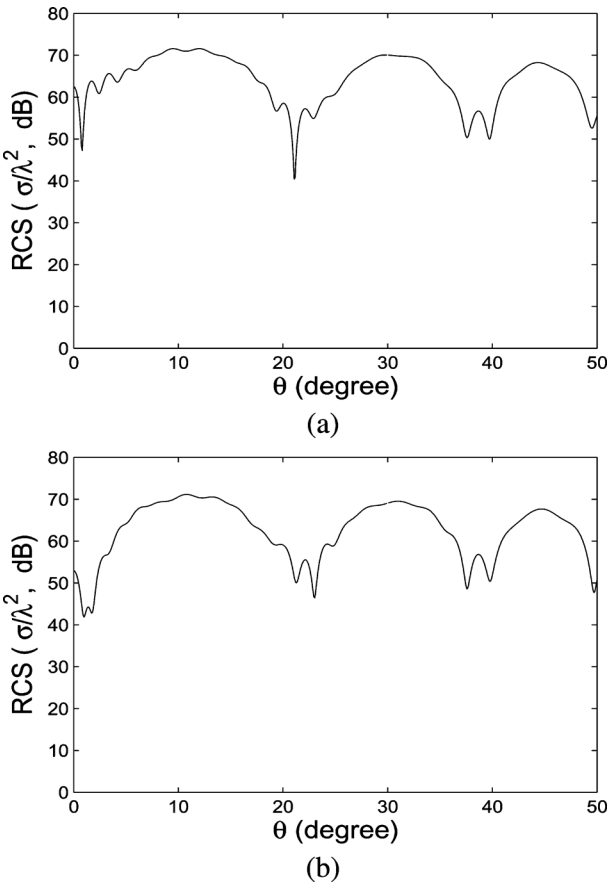

Fig. 5. RCS of the cavity with size $W_1 = 20\lambda$, $W_2 = 60\lambda$, and $W_3 = 50\lambda$. (a): $\hat{\phi}\hat{\phi}$ polarization; (b): $\hat{\theta}\hat{\theta}$ polarization.

V. Conclusion

A new mode matching method is presented for the scattering from three dimensional large cavities. The method is based on the periodic extension of the electric field over the cavity aperture to the whole ground plane. It shares the low computational cost with the usual modal approach by solving only the coefficients of the modes. In addition, the method leads to better accuracy for larger cavities than it is for the smaller cavities, which is well suited for the computation of the scattering from very large cavities. In the extreme case when the size of the cavity aperture goes to infinity, the numerical solution converges to the exact solution.

Appendix
Derivation of the Formula (5)

The Fourier transform of the scattered field $E^{s,+}$ are the outgoing propagation modes expressed by

$$\widehat{E_j^{s,+}}(\xi_1,\xi_2,z) = e^{i\sqrt{k^2-\xi_1^2-\xi_2^2}z}\widehat{E_j^{s,+}}(\xi_1,\xi_2,0), \quad \text{for } j = x,y,z. \tag{16}$$

It is easily seen that

$$\frac{\partial \widehat{E_z^{s,+}}(\xi_1,\xi_2,z)}{\partial z} = i\sqrt{k^2-\xi_1^2-\xi_2^2}\,\widehat{E_z^{s,+}}(\xi_1,\xi_2,z). \tag{17}$$

On the other hand, by the application of the Gauss's law,

$$\begin{aligned}\widehat{\frac{\partial E_j^{s,+}}{\partial z}} &= \frac{1}{2\pi}\int_{\mathbb{R}^2}\frac{\partial E_z^{s,+}}{\partial z}e^{-i(x\xi_1+y\xi_2)}dxdy \\ &= -\frac{1}{2\pi}\int_{\mathbb{R}^2}\left(\frac{\partial E_x^{s,+}}{\partial x}+\frac{\partial E_y^{s,+}}{\partial y}\right)e^{-i(x\xi_1+y\xi_2)}dxdy \\ &= -i\left(\xi_1\widehat{E_x^{s,+}}(\xi_1,\xi_2,z)+\xi_2\widehat{E_y^{s,+}}(\xi_1,\xi_2,z)\right). \end{aligned}\tag{18}$$

Therefore, (16)–(18) implies that

$$\begin{aligned}\widehat{E_z^{s,+}}(\xi_1,\xi_2,z) &= -\frac{1}{\sqrt{k^2-\xi_1^2-\xi_2^2}}[\xi_1\widehat{E_x^{s,+}}(\xi_1,\xi_2,z) \\ &\quad +\xi_2\widehat{E_y^{s,+}}(\xi_1,\xi_2,z)] \\ &= -\frac{1}{\sqrt{k^2-\xi_1^2-\xi_2^2}}[\xi_1\widehat{E_x^{s,+}}(\xi_1,\xi_2,0) \\ &\quad +\xi_2\widehat{E_y^{s,+}}(\xi_1,\xi_2,0)]e^{i\sqrt{k^2-\xi_1^2-\xi_2^2}z}.\end{aligned}$$

By taking the inverse Fourier transform and noting that $E_x^{s,+}(x,y,0) = \mathcal{T}_0(E_x^-(x,y,0))$, $E_y^{s,+}(x,y,0) = \mathcal{T}_0(E_y^-(x,y,0))$, we arrive at formula (5).

References

[1] A. Altintas, P. Pathak, and M. Liang, "A selective modal scheme for the analysis of EM coupling into or radiation from large open-ended waveguides," *IEEE Trans. Antennas Propagat.*, vol. 36, pp. 84–96, 1988.

[2] H. Ammari, G. Bao, and A. Wood, "A cavity problem for Maxwell's equations," *Meth. Appl. Anal.*, vol. 9, pp. 249–260, 2002.

[3] G. Bao and W. Sun, "A fast algorithm for the electromagnetic scattering from a large cavity," *SIAM J. Sci. Comput.*, vol. 27, pp. 553–574, 2005.

[4] G. Bao and W. Zhang, "An improved mode-matching method for large cavities," *IEEE Antennas Wireless Propagat. Lett.*, vol. 27, pp. 393–396, 2005.

[5] R. Burkholder and P. Pathak, "Analysis of EM penetration into and scattering by electrically large open waveguide cavities using Gaussian beam shooting," *Proc. IEEE*, vol. 79, pp. 1401–1412, 1991.

[6] C. Huang, "Simple formula for the RCS of a finite hollow circular cylinder," *Electron. Lett.*, vol. 19, pp. 854–856, 1983.

[7] P. Huddleston, "Scattering from conducting finite cylinders with thin coatings," *IEEE Trans. Antennas Propagat.*, vol. 35, pp. 1128–1136, 1987.

[8] J. Jin, "A finite element-boundary integral formulation for scattering by three-dimensional cavity-backed apertures," *IEEE Trans. Antennas Propagat.*, vol. 39, pp. 97–104, 1991.

[9] J. Jin, *The Finite Element Method in Electromagnetics*, 2nd ed. New York: Wiley, 2002.

[10] J. Jin, J. Liu, Z. Lou, and S. T. Liang, "A fully high-order finite-element simulation of scattering by deep cavities," *IEEE Trans. Antennas Propagat.*, vol. 51, pp. 2420–2429, 2003.

[11] T. Johnson and D. Moffatt, "Electromagnetic scattering by open circular waveguide," *Radio Sci.*, vol. 17, pp. 1547–1556, 1982.

[12] C. Lee and S. Lee, "RCS of a coated circular waveguide terminated by a perfect conductor," *IEEE Trans. Antennas Propagat.*, vol. 35, pp. 391–398, 1987.

[13] H. Ling, R. Chou, and S. Lee, "Shooting and bouncing rays: Calculating the RCS of an arbitrarily shaped cavity," *IEEE Trans. Antennas Propagat.*, vol. 37, pp. 194–205, 1989.

[14] H. Ling, S. Lee, and R. Chou, "High-frequency RCS of open caivties with rectangular and circular cross sections," *IEEE Trans. Antennas Propagat.*, vol. 37, pp. 648–654, 1989.

[15] J. Liu and J. Jin, "A special higher order finite-element method for scattering by deep cavities," *IEEE Trans. Antennas Propagat.*, vol. 48, pp. 694–703, 2000.
[16] P. Miller, *Applied Asymptotic Analysis*, ser. Graduate Studies in Mathematics. Providence, RI: American Mathematical Society, 2006, vol. 75.

Gang Bao received the B.S. degree in computational mathematics from Jilin University, Changchun, China, in 1985 and the Ph.D. degree in applied mathematics from Rice University, Houston, TX, in 1991.

After spending five years at University of Florida, Gainsville, as Assistant and later Associate Professor, he has been Professor of Mathematics at Michigan State University, East Lansing, since 1999. He is also the founding director of the Michigan Center for Industrial and Applied Mathematics (MCIAM) since 2006, and a National Chair Professor at Zhejiang University, Hangzhou, China, since 2010.

He has published over 125 papers in the general areas of applied mathematics, particularly modeling, analysis, and computation of diffractive optics, nonlinear optics, near-field and nano-optics, and electromagnetics; inverse and design problems for partial differential equations; numerical analysis; multiscale, multi-physics scientific computing. He has served on the editorial boards of eight journals on applied mathematics and many panels. Over the past five years, he has organized six international conferences and given over 60 invited talks. His list of awards include Cheung Kong Scholar in 2001, the 2003 Feng Kang Prize of Scientific Computing, Distinguished Overseas Young Researcher Award, National Science Foundation of China in 2004, and a University Distinguished Faculty Award, Michigan State University in 2007.

Jinglu Gao was born in Changchun, China, in 1982. She received the B.S., M.S., and Ph.D. degrees majoring in computational mathematics from Jilin University, Changchun, China, in 2005, 2007, and 2011, respectively. From 2008 to 2010 she studied at Michigan State University, East Lansing, as an exchange Ph.D. degree student.

She is currently an Editor working at the mathematical Journal *Communications in Mathematical Research*.

Junshan Lin received the B.S. and M.S. degrees in computational mathematics from Jilin University, Changchun, China, and Fudan University of China, Shanghai, respectively, and the Ph.D. degree in applied mathematics from the Michigan State University, East Lansing, in 2011.

Currently, he is a Postdoctoral Associate at the Institute for Mathematics and its Applications. His research interests include wave propagation, inverse problems, numerical analysis and scientific computation.

Weiwei Zhang received the B.S. and M.S. degrees in mathematics from Jilin University, Changchun, China, in 1997 and 2000, respectively, and the Ph.D. degree in applied mathematics from Michigan State University, East Lansing, in 2006. Her research interest is in numerical analysis, scientific computation, and applications.

Since August 2006, she has been an Assistant Professor in the mathematics department at King's College, Wilkes-Barre, PA.